

Seismic Microzonation of Toba Lake Region Using Microtremor Analysis

Fauzan Surya Nanda^{1*}, Furqon Raharjo², Suaidi Ahadi²

¹ Department of Physics, Universitas Andalas, Padang 25163, Indonesia

² Agency of Meteorology, Climatology, and Geophysics, 10720, Indonesia

(Received October 21, 2026; revised February 09, 2026; accepted February 12, 2026; published online April 18, 2026)

The Toba Lake region, characterized by complex volcanic and tectonic history, represents a significant seismic hazard zone due to its proximity to the active Sumatra Fault System and heterogeneous geological conditions. This study applies the Horizontal to Vertical Spectral Ratio (HVSr) method using microtremor data to assess seismic vulnerability across the region. Three-component microtremor recordings from 29 stations were analyzed to derive key seismic parameters including predominant frequency (f_0), amplification factor (A_0), dominant period (T_0), and seismic vulnerability index (K_g). The results reveal significant spatial variations in seismic hazard parameters, with high vulnerability zones concentrated in the central and southern areas, characterized by low predominant frequencies (0.6-1.2 Hz), high amplification factors (up to 12.0), long dominant periods (1.2-2.1 seconds), and elevated vulnerability indices ($K_g > 8.0$). These zones correspond to Quaternary alluvial deposits with soft, unconsolidated sediments. Conversely, northern and northwestern regions exhibit lower vulnerability with high predominant frequencies (>2.0 Hz), low amplification factors (<4.0), short dominant periods (<0.6 seconds), and reduced vulnerability indices ($K_g < 3.0$), correlating with consolidated Miocene volcanic rocks. Critical high-risk areas include measurement points LT34, LT14, LT17, LT21, and LT49, while point LT20 in Tarutung, located along the Sumatra Fault Zone, demonstrates the compound effect of active tectonics and soft geological conditions. The resulting microzonation maps provide a regional-scale framework for seismic hazard identification and disaster risk mitigation planning, and can serve as a reference for prioritizing areas requiring more detailed, site-specific investigations.

Keywords: Seismic Vulnerability Index, HVSr, Microtremor



This is an open access article under the [CC BY-NC](https://creativecommons.org/licenses/by-nc/4.0/) license.
Copyright © 2025 by Author. Published by Physical Society of Indonesia

1. INTRODUCTION

The Toba Caldera, formed by a supervolcanic eruption approximately 74,000 years ago. This caldera now constitutes the world's largest volcanic lake and preserves complex geological history with high natural hazard potential (Aldiss & Ghazali, 1984). Beyond its scientific value, the region holds strategic socio-economic importance as a center for tourism activities and transportation for North Sumatra communities (Arrasyid et al., 2024). Infrastructure development, population density, and tourism sector growth render this area vulnerable to geological disaster impacts (Grutas et al., 2025). Consequently, this region requires comprehensive disaster mitigation studies based on geological and geophysical data (Wibowo et al., 2023).

Tectonically, the Lake Toba area lies within the influence of the active Sumatra Fault System, creating high potential for seismic events (Asnawi et al., 2022). Additionally, volcanic sediment deposits from past eruptions generate heterogeneous surface geological conditions that potentially cause local seismic wave amplification (Darmawan et al., 2021). Thick sediment layers can resonate with natural building frequencies, increasing damage risk during earthquakes (Z. Chen et al., 2023). This phenomenon was observed in the 2018 Palu and 2006 Yogyakarta earthquakes, where damage was more influenced by local soil conditions than distance from earthquake sources (Eka Setiawan et al., 2024).

Understanding local soil characteristics becomes crucial for earthquake disaster mitigation efforts (Hakim, 2019). The microtremor method with Horizontal to Vertical Spectral Ratio (HVSr) is

*Contact Author: fauzansuryananda@gmail.com

widely utilized as it is non-destructive, efficient, and applicable in densely populated areas (Yulianto & Yuliyanto, 2023). In Indonesia, the method has been successfully applied for site response analysis along active fault zones such as the Kaligarang Fault. HVSR enables identification of important parameters including soil predominant frequency (f_0), dominant period (T_0), seismic vulnerability index (K_g), and amplification factor (A_0) earthquakes (Z. Chen et al., 2023).

Previous research has demonstrated HVSR method effectiveness across various geological and seismotectonic contexts (Akkaya, 2015). Studies have shown that younger geological formations tend to be more susceptible to seismic wave amplification, with areas containing thick sediment layers (>15 m) and low f_0 values (<1 Hz) exhibiting high K_g values and significant amplification potential. However, limited research has specifically mapped seismic vulnerability using HVSR methods in the Lake Toba region (Eka Setiawan et al., 2024) despite its complex geological characteristics and high anthropogenic activity, particularly in densely populated zones such as Balige, Parapat, and Haranggaol (Grutas et al., 2025).

This study aims to apply HVSR methodology to obtain maps of predominant frequency (f_0), dominant period (T_0), and seismic vulnerability index (K_g), as foundation for identifying earthquake-prone zones in the Lake Toba region (Chen et al., 2023). The findings are expected to contribute to more adaptive development planning and earthquake disaster risk mitigation based on geophysical data (Wibowo et al., 2023).

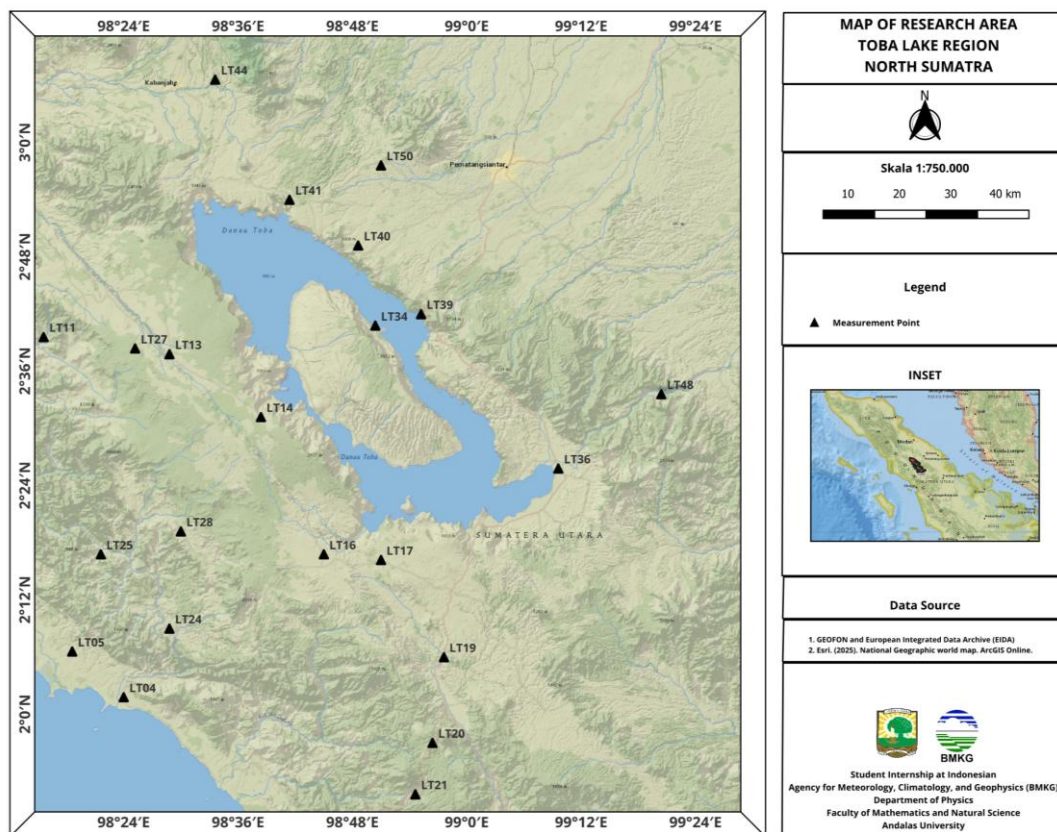


Figure 1 Map of the study area showing the locations of microtremor measurement points.

2. DATA AND METHOD

2.1 Data

This study utilized secondary data consisting of three-component microtremor recordings obtained from GEOFON and European Integrated Data Archive (EIDA) open repositories. A total of 29 stations were analyzed, with data collected during September 2008. The use of this dataset is considered

appropriate because ambient seismic noise is dominated by natural sources and is assumed to be stationary over long time periods, particularly for regional-scale site response assessment. The measurement sites are mostly located in areas with limited anthropogenic activity, minimizing the influence of non-seismic noise. The microtremor recordings include vertical (Z), north-south (N), and east-west (E) components, which are essential for HVSr analysis. Data processing was conducted in accordance with the SESAME (2004) guidelines for H/V spectral ratio analysis. The time-series records were detrended, corrected for baseline offsets, and divided into stationary time windows. Windows affected by transient noise were excluded prior to spectral analysis. This procedure ensures the reliability of the estimated predominant frequency (f_0) and prevents artificial overestimation of the amplification factor (A_0) and seismic vulnerability index (K_g).

2.2 Area of Study

The research area is geographically located in the Lake Toba region, North Sumatra, Indonesia, as shown in Figure 1 *Map of Research Area Around Lake Toba*. It extends from approximately 1°48'N to 3°00'N latitude and 98°12'E to 99°12'E longitude, covering both the western and eastern margins of the Toba Caldera.

The distribution of microtremor measurement points across the caldera and its surroundings was designed to capture these spatial variations and to provide a regional-scale characterization of site response. Consequently, the study area offers an appropriate setting for seismic microzonation based on ambient vibration analysis, particularly for identifying zones with potentially higher seismic vulnerability (Nakamura, 1989).

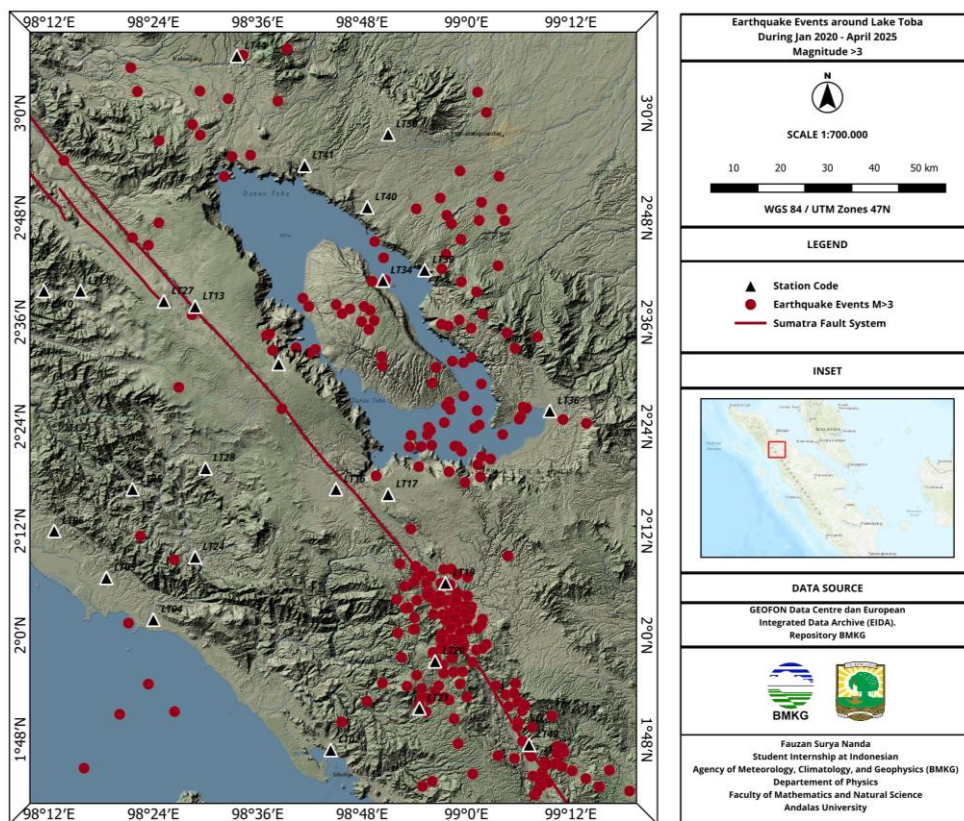


Figure 2 Seismicity map showing earthquake events around Lake Toba from January 2020 to April 2025.

2.3 Seismicity and Tectonics

The seismic and tectonic characteristics of the Lake Toba region, which reflect a complex interplay between volcanic and tectonic processes, are illustrated in Figure 2. This map integrates earthquake distribution data with regional geological structures, highlighting seismic events ($M > 3$) recorded between January 2020 and April 2025. These data, sourced from BMKG, are plotted alongside

the Sumatra Fault System and regional seismic stations. This visual framework is crucial for understanding how active tectonic features, such as the Sumatra Fault and surrounding crustal fractures, influence the spatial distribution of seismicity in northern Sumatra.

The tectonic and volcanic complexity of Lake Toba is illustrated in the *Earthquake Events* map, which plots seismicity ($M > 3$) from 2020 to 2025 using BMKG data. The earthquake distribution aligns closely with major fault systems like the Sumatra Fault and Renun Fault, indicating active tectonic deformation. Lake Toba lies above the subducting Indo-Australian plate and is affected by the oblique convergence with the Eurasian plate. Hutchings and Mooney (2021) noted that most earthquakes in this region are shallow (≤ 70 km), but intermediate and deep events trace the subduction geometry. Meanwhile, Simanjuntak et al. (2022) identified a *slab gap* beneath Toba, formed due to the oblique subduction of the Investigator Fracture Zone (IFZ). This fracture zone, though not seen on the surface, generates complex seismic patterns and may involve a possible *slab tear*. Hypocenter relocation confirms that seismic events cluster along a dipping structure consistent with the IFZ trajectory, reinforcing the idea of segmented slab subduction. This unique tectonic configuration contributes to Toba's persistent seismicity and underscores the region's geological hazards.

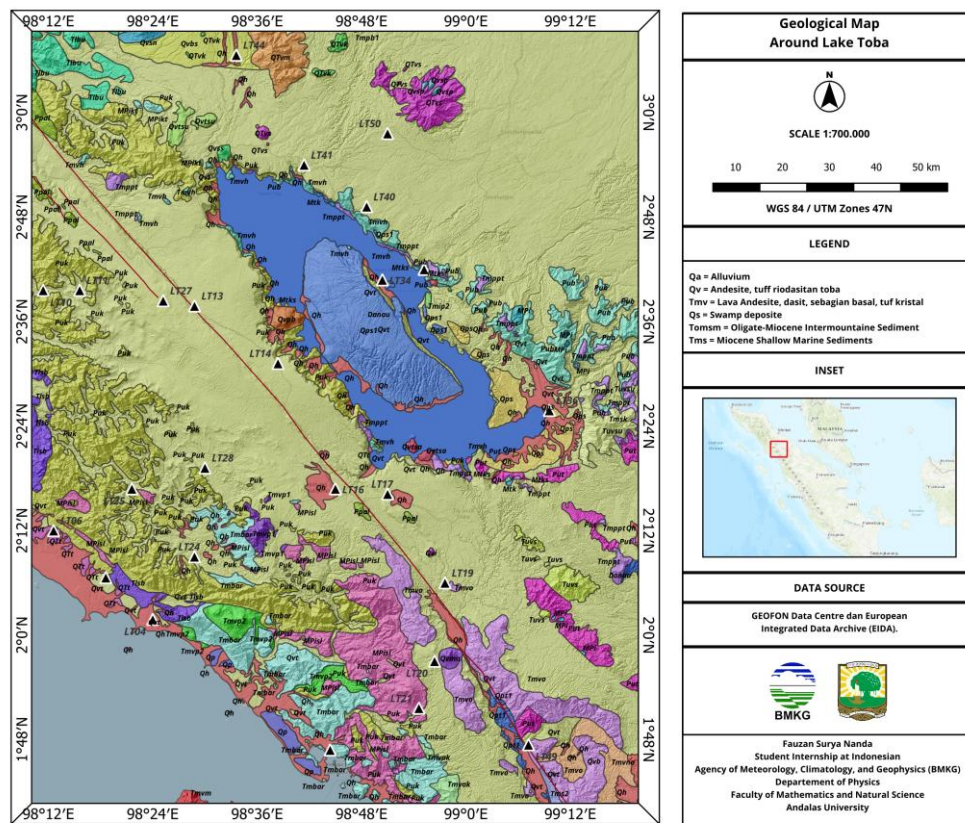


Figure 3 Geological map around Lake Toba.

2.4 Geology

The geological conditions of Lake Toba, which reflect its complex volcanic and tectonic history, are illustrated in Figure 3 This geological map provides a comprehensive overview of the lithological units and structural features that have shaped the region, including remnants of the Toba Caldera, volcanic deposits, and fault systems associated with the active Sumatra Fault Zone. Understanding these geological characteristics is essential for interpreting subsurface conditions, assessing geohazards, and supporting further geophysical analyses in the area.

The geological conditions of the Lake Toba area can be further detailed by examining the specific geological units mapped in the region (Aldiss & Ghazali, 1984). Key units that compose the

Lake Toba area and its surroundings include Qa (Alluvium), representing unconsolidated sediments transported and deposited by water, indicating ongoing modern sedimentary processes. The presence of Qv (Andesite, Toba Rhyodacitic Tuff) signifies volcanic rocks directly linked to the Toba volcanic activity, highlighting the dominant volcanic nature of the area. Additionally, Tmv (Andesite Lava, Dacite, partly Basalt, Crystal Tuff), consisting of a variety of igneous volcanic rocks, points to a complex and diverse history of volcanism. Qs (Swamp Deposits) refers to marshy area deposits, suggesting the existence of past or present wetlands around Lake Toba. Furthermore, Tomsm (Oligocene-Miocene Intermontane Sediments) indicates sedimentary basins formed between mountainous topographies during the Oligocene to Miocene epochs. Lastly, Tms (Miocene Shallow Marine Sediments) suggests that parts of the area were characterized by a shallow marine environment during the Miocene before undergoing uplift and subsequent geological process (Gafoer et al, 1996).

2.5 Horizontal to Spectral Vertical Ration (HVSr)

HVSr, pioneered by Nakamura (1989), is a widely used seismic microzonation technique for evaluating the influence of local soil conditions on earthquake ground motion amplification and supporting urban-scale seismic microzonation studies (Gosar, 2017). The method involves calculating the spectral amplitude ratio between the average horizontal components and the vertical component of microtremor signals (Konno & Ohmachi, 1998). The resulting HVSr curve provides the ground's resonance behavior, where the peak frequency corresponds to the site's dominant frequency (f_0). The HVSr ratio is formally expressed as

$$HVSr = \sqrt{\frac{(A_{(N-S)}(f))^2 + (A_{(W-E)}(f))^2}{(A_{(V)}(f))}} \tag{1}$$

where $A_{(N-S)}$ and $A_{(W-E)}$ are the amplitude spectra of the North-South and West-East horizontal components, and $A_{(V)}$ is the amplitude spectrum of the vertical component. This approach is highly reliable for identifying soft sediment layers and their thickness (Nugroho et al., 2023).

2.6 Seismic Hazard Parameter

2.6.1 Natural Frequency

The natural frequency, commonly denoted as the peak frequency of the HVSr curve, is a key parameter in characterizing local site conditions. It represents the fundamental frequency at which ground layers resonate due to incoming seismic energy, particularly in soft sedimentary basins overlaying bedrock (Alonso-Pandavenes et al., 2023) Determining this frequency is essential for assessing potential resonance with structures during seismic events. To calculate the natural frequency, the following equation is used :

$$f_0 = \frac{v_s}{4h} \tag{2}$$

where f_0 denotes the natural frequency (Hz), v_s represents the average shear wave velocity of the sediment layer (m/s), and h is the thickness of the soft sediment layer (m). This relation assumes a two-layer system, where surface soft sediments overlay a stiffer substratum.

Table 1 . Definition of site classification for this project (Grajales-Saavedra et al, 2023).

Site Class	Predominant Frequency (Hz)
rock/stiff soil	$f_0 > 5$
rigid soil	$2.5 < f_0 \leq 5$
semi-rigid soil	$1.6 < f_0 \leq 2.5$
soft soil	$f_0 \leq 1.6$

2.6.2 Amplification factor

The amplification factor reflects the extent to which seismic waves are intensified due to local soil conditions. It is derived from the HVSr curve as the maximum ratio of horizontal to vertical spectral

amplitudes (Asnawi et al., 2022). The amplification factor can be calculated using the following equation:

$$A_0 = \frac{cb}{c_s} \quad (3)$$

with A_0 representing the amplification factor, cb denoting the shear wave velocity (v_s) in the basement layer (m/s), and c_s indicating the shear wave velocity (v_s) in the weathered layer (m/s).

The dominant period is the inverse of the natural frequency and indicates the time at which the soil profile oscillates most significantly during ground shaking. It is particularly relevant in assessing the resonance risk between site conditions and building structures (Grutas et al., 2025). The dominant period is calculated using the following equation:

$$T_0 = \frac{1}{f_0} \quad (4)$$

where T_0 is the dominant period (s) and f_0 is the natural frequency (Hz). This simple yet important relationship allows for the identification of potentially vulnerable buildings whose natural periods are close to that of the ground, increasing the risk of resonance during earthquakes (Asnawi et al., 2022).

Table 2 . Definition of site classification for this project (Savaadra, 2023).

Site Class	Dominant Period (s)
SC I	$T < 0.2$
SC II	$0.2 \leq T < 0.4$
SC III	$0.4 \leq T < 0.6$
SC IV	$T \geq 0.6$

2.6.3 Seismic Vulnerability Index

The Seismic Vulnerability Index (K_g) is a composite indicator that integrates the amplification factor and natural frequency to assess site susceptibility to seismic damage. It has been increasingly used in urban seismic microzonation and disaster risk mitigation efforts (Wibowo et al., 2023). To compute the vulnerability index, the calculated using the following equation:

$$K_g = \frac{A_0^2}{f_0} \quad (5)$$

In this expression, K_g is the vulnerability index, A_0 is the amplification factor, and f_0 is the natural frequency. A higher K_g value indicates greater seismic vulnerability, often associated with soft, thick sediment layers exhibiting both high amplification and low frequency (Arrasyid et al., 2024).

3. RESULTS AND DISCUSSION

3.1 Horizontal to Spectral Vertical Ration (HVSr)

The H/V spectral ratio (HVSr) curves obtained from ambient noise recordings at selected measurement points around Lake Toba are presented in Figure 4 These curves illustrate the frequency-dependent behavior of seismic wave amplification at each site and serve as the basis for identifying predominant frequencies, amplification factors (Z. Chen et al., 2023).

The curve shown in Figure 4 exhibits a sharp and distinct peak, indicating a strong impedance contrast between two subsurface layers. The measured predominant frequency (f_0) reflects the depth of the reflection interface, typically representing the boundary between sedimentary layers and the underlying bedrock. A lower f_0 value (longer period) suggests a deeper boundary, indicating thicker sedimentary deposits. Conversely, a higher f_0 value implies a shallower boundary, associated with thinner sediment layers. In addition, the amplification factor (A_0) on the HVSr curve indicates the extent to which surface waves are amplified by subsurface structures. Higher A_0 values correspond to greater impedance contrasts between layers, which are influenced by differences in density and seismic wave velocity across each layer.

A curve featuring two distinct peaks (double peak) suggests the presence of impedance contrasts at multiple depths, meaning that surface waves are traversing several layers with differing physical properties. For instance, the surface layer may consist of loose or unconsolidated sediments, followed by a denser sediment layer, and finally, a relatively rigid bedrock at greater depth. Meanwhile, a broad

peak curve is typically associated with inclined bedrock morphology—such as in concave valley structures—or lateral variations in the sediment-bedrock interface. This type of topology reflects the geological complexity of the subsurface structure, both vertically and laterally.

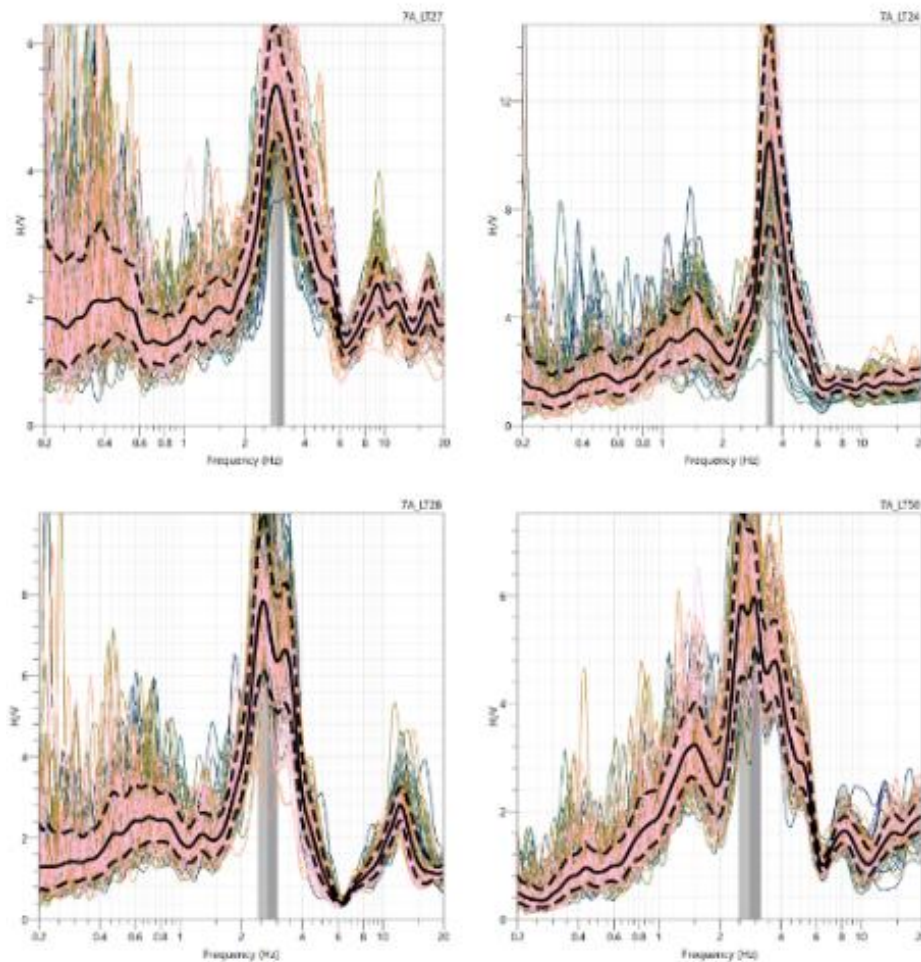


Figure 4 The H/V curve around Lake Toba.

3.2 Seismic Hazard Parameter

3.2.1 Natural Frequency

The microzonation map of predominant frequency around Lake Toba as shown in Figure 5 reveals significant spatial variations, with observed frequencies generally ranging from approximately 0.6 Hz (bluish colors) to over 2.1 Hz (red colors).

The predominant frequency (f_0) is a key parameter that reflects the natural frequency at which soil layers resonate most strongly with seismic waves. Based on the analysis results, areas with low predominant frequency (indicated by bluish to yellow colors) are prominently observed in the central and southern parts of the study area, particularly around the immediate vicinity of Lake Toba and extending southwards. These areas likely correspond to thicker sediment basins or soft, unconsolidated deposits. For instance, points LT34, LT14, LT17, LT21, and LT49 show lower predominant frequencies. According to Table 1, these low frequencies typically indicate soft to medium soil conditions. Conversely, areas with high predominant frequency (indicated by orange to dark red colors) tend to be situated in locations with stiffer soil layers or shallow bedrock, such as the regions to the northwest (e.g., LT10, LT11) and isolated spots like LT44 and LT36. These higher frequencies, as per Table 1, are indicative of stiff soil or rock sites.

presence of soft, unconsolidated surface materials. Interestingly, point LT20, situated in the Tarutung area, also shows a notably high amplification factor. This location is particularly important as it lies directly along the Sumatra Fault Zone (SFZ)—a major active strike-slip fault system in the region. When correlated with geological data, the Tarutung area is found to be underlain by Quaternary alluvial deposits, consisting of soft, loose sediments with poor compaction. These geological conditions, combined with tectonic activity from the SFZ, contribute to significant site effects and a heightened potential for ground shaking amplification (Gafoer et al, 1996).

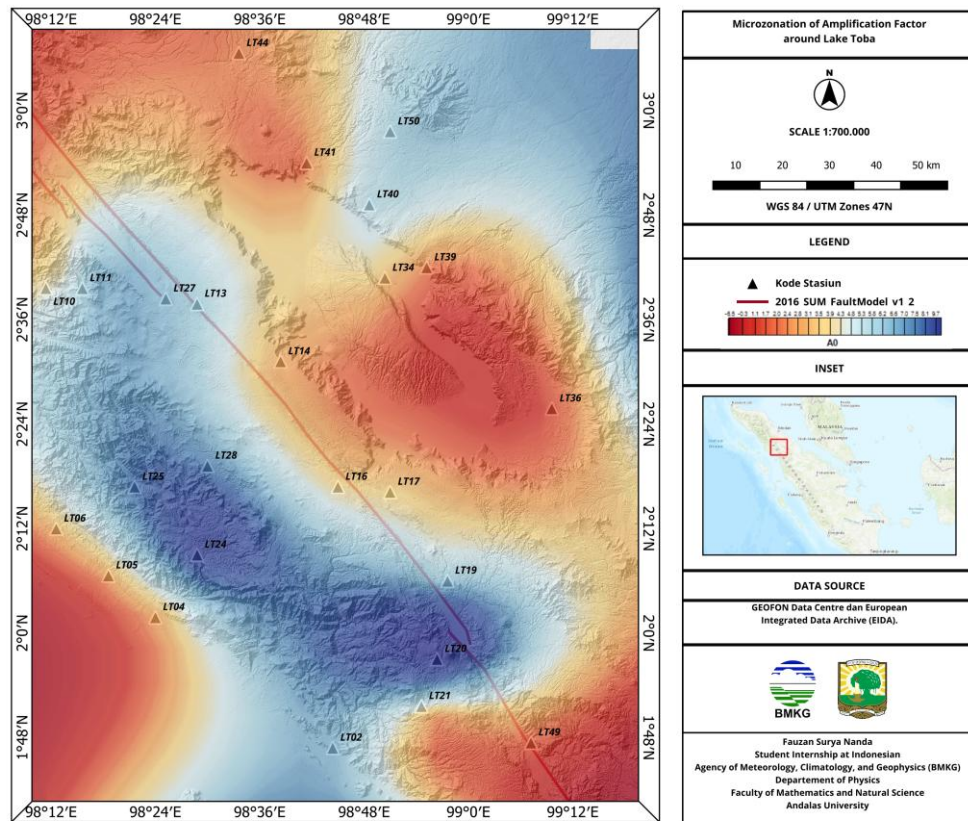


Figure 6 The microzonation of amplification factor around Lake Toba.

3.2.3 Dominant Period

The dominant period (τ_0) map around Lake Toba as shown in Figure 7 reveals periods generally ranging from approximately 0.6 seconds (bluish colors) to over 2.1 seconds (dark red colors). The dominant period is particularly relevant for assessing the potential resonance with structures of varying height.

The dominant period is the inverse of the predominant frequency (Equation 3) and represents the most significant oscillation time of the soil profile during shaking. Areas with long dominant periods (displayed in dark red colors) are conspicuously present in the central and southern parts of the study area, precisely mirroring the regions with low predominant frequencies and high amplification factors (e.g., LT34, LT14, LT17, LT21, LT49). According to Table 2 (Classification Table for Dominant Period), these long periods typically indicate soft to very soft soil conditions. These zones indicate the presence of thick and soft sediment layers that will oscillate more slowly, typically for periods ranging from 1.2 to 2.1 seconds or higher. These areas have the potential to cause resonance with high-rise buildings that have similar natural periods, increasing the risk of structural damage. Conversely, areas with short dominant periods (displayed in bluish colors), such as the northwestern and scattered northern locations (e.g., LT10, LT11, LT44, LT36), indicate stiffer soil layers or shallow bedrock, which tend to resonate with low-rise buildings (periods typically below 0.6 seconds). Based on Table 2, these shorter periods are characteristic of stiff soil or rock sites.

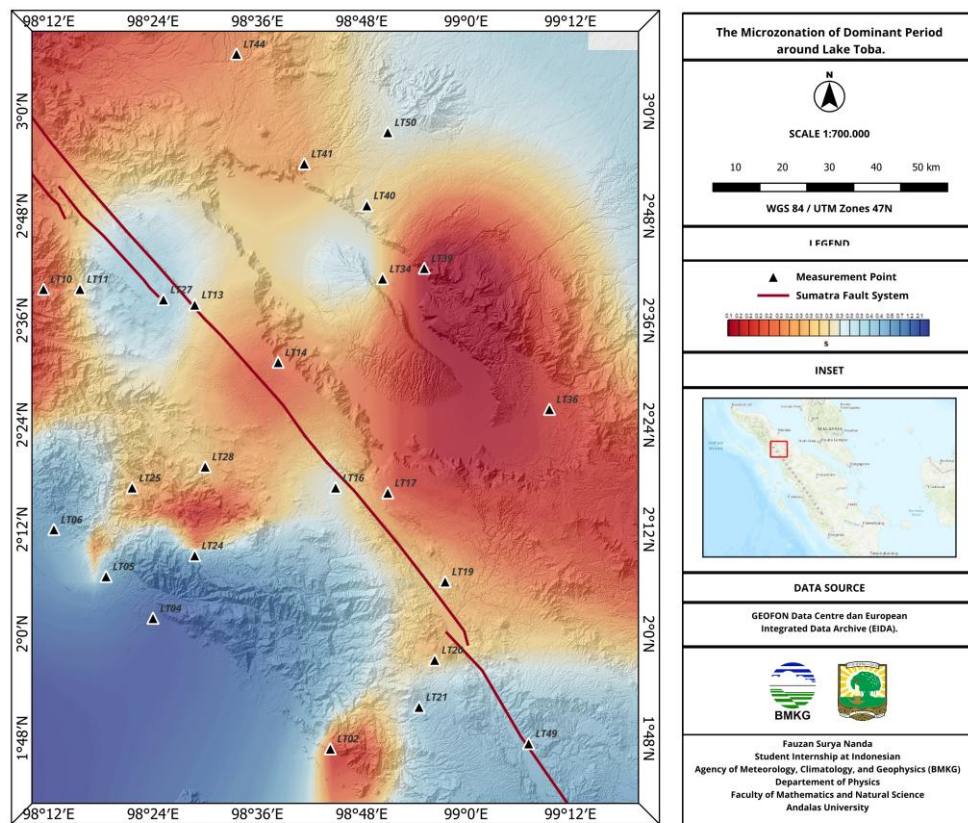


Figure 7 The microzonation of dominant period around Lake Toba

A notable example is point LT39 in the Parapat area, which exhibits the shortest dominant period across the study area. When correlated with the geological map, this point lies within the Tmv unit, representing Miocene volcanic rocks composed of andesitic to dacitic lavas, basalt, breccia, agglomerate, and volcanoclastic deposits. These volcanic rocks are known for their high rigidity and shallow depth, resulting in a stiff response to seismic waves and hence, a very short dominant period. This correlation confirms that consolidated and coherent lithologies, such as those in the Tmv unit, contribute to rapid ground response during shaking. In contrast, the longest dominant periods were observed in the central part of Samosir Island and are also widespread along the southern shoreline of Lake Toba. These zones are underlain by the Qa unit (*Quaternary alluvium*), which consists of soft, unconsolidated deposits such as clay, silt, sand, and gravel (Gafoer et al, 1996). The thick and low-density nature of these sediments causes them to resonate at longer periods. Their widespread presence, especially in the southern basin and coastal margins of the lake, highlights a broader zone of potential seismic hazard due to extended shaking durations and greater likelihood of resonance with taller buildings (Gafoer et al 1996).

3.2.4 Seismic Vulnerability Index

The seismic vulnerability index (*Kg*) map around Lake Toba (Figure 8), values typically range from approximately 3.0 (bluish colors) to over 12.0 (dark red colors).

High seismic vulnerability index values (indicated by bluish colors) are prominently concentrated in the central and southern parts of the study area, specifically around the lake's southern shores and extending towards the south, encompassing points like LT34, LT14, LT17, LT21, and LT49. These zones are identified as most susceptible to earthquake damage. These areas typically have a critical combination of high amplification and low predominant frequency (or long dominant period), indicating soft, thick soil layers with a high potential for ground motion amplification. The *Kg* values in these regions can reach up to 12.0 or higher. Conversely, areas with low seismic vulnerability index

(indicated by red colors) are primarily located in the northern and northwestern regions (e.g., LT10, LT11, LT44, LT36), indicating more stable soil conditions and less susceptibility to seismic amplification, with K_g values generally below 3.0. From a geological perspective, low K_g values, generally below 1.0, are found in the northern and northwestern regions (e.g., LT10, LT11, LT44, LT36), where soils are stiffer and bedrock is shallower. These areas correlate with the Tmv unit (Miocene volcanic rocks), comprising andesite, dacite, and breccia—lithologies that produce lower amplification and shorter response periods (Gafoer et al, 1996).

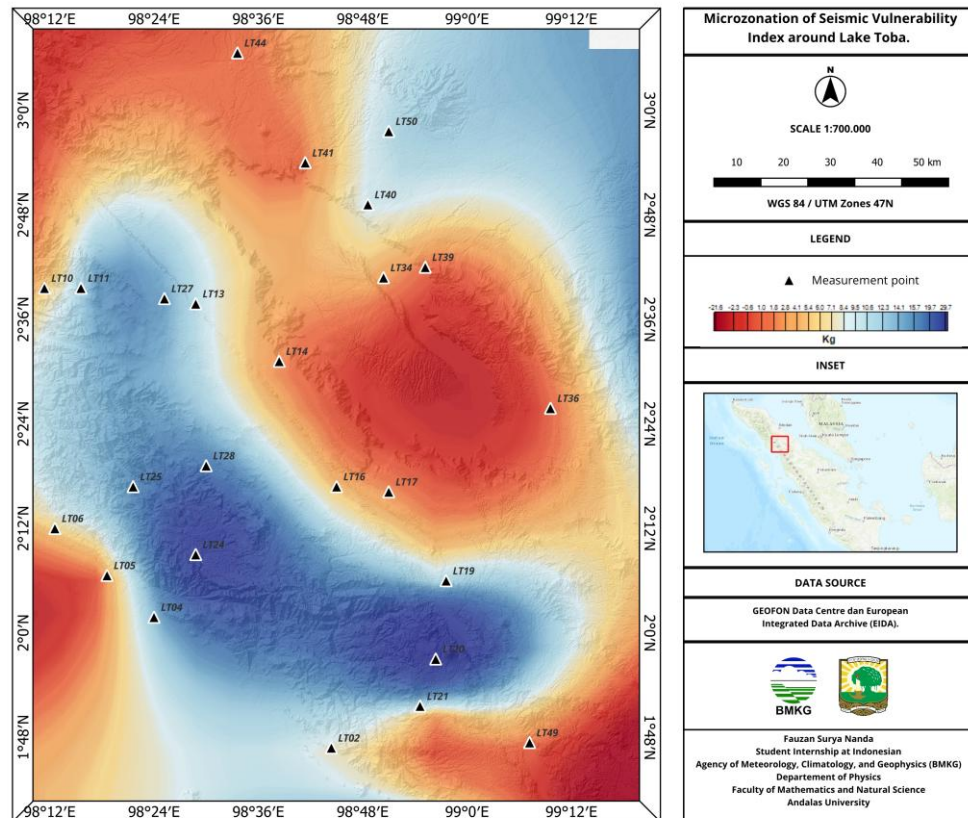


Figure 8 The microzonation of seismic vulnerability index around Lake Toba

3.2.5 Distribution of H/V Spectral Ratio

To assess variability of subsurface conditions, the results of the H/V spectral ratio analysis for each measurement station are summarized in Table 3. Key parameters derived from the analysis include the predominant frequency of the subsoil, the corresponding period (dominant period), the peak amplitude of the H/V curve, and the seismic vulnerability index. Results obtained in the H/V spectral ratio analysis for each station are presented in Table 3.

It should be noted that the seismic microzonation maps presented in this study are derived from 29 microtremor measurement stations distributed across the Lake Toba region. Given the large spatial extent and geological complexity of the study area, the relatively low station density may introduce spatial aliasing effects, particularly in areas characterized by strong lateral variations in lithology and sediment thickness. Consequently, the interpolated microzonation patterns should be interpreted as first-order regional trends rather than detailed representations of local site conditions. Despite this limitation, the observed spatial consistency between low predominant frequency, high amplification factor, elevated seismic vulnerability index, and Quaternary alluvial deposits suggests that the HVSR results capture the dominant regional site response characteristics. The maps therefore provide a useful framework for identifying zones of relatively higher and lower seismic hazard at a regional scale, while acknowledging that finer-scale variations may not be fully resolved without higher station density.

Table 3 . Value of the Predominant frequency (f_0), amplification factor (A_0), dominant period (T_0), and seismic vulnerability index (K_g) obtained in each of the 29 stations

Station	f_0 (Hz)	A_0	T_0 (s)	K_g
LT01	2.3253	7.2872	0.4300	22.83717535
LT02	5.6571	6.6578	0.1767	7.835516579
LT04	0.4444	2.4676	2.2502	13.70173213
LT05	8.0901	2.6719	0.1236	0.88244269
LT06	1.4372	3.309	0.6957	7.618620234
LT09	6.4779	4.1602	0.1543	2.671739922
LT10	6.3448	2.9381	0.1576	1.360552202
LT11	3.1366	7.1699	0.3188	16.38955111
LT13	3.4626	6.0336	0.2888	10.51358198
LT14	5.2871	2.4309	0.1891	1.117677897
LT16	3.1365	3.6368	0.3188	4.216902356
LT17	5.185	3.9227	0.1928	2.967709796
LT19	3.6394	5.888	0.2747	9.525895477
LT20	3.9239	12.624	0.2548	40.61595619
LT21	2.4983	2.3599	0.4002	2.229167038
LT24	3.5289	10.179	0.2833	29.36504069
LT25	3.8949	7.8862	0.2567	15.96758593
LT27	2.7087	6.4175	0.3691	15.20445463
LT28	3.055	7.4004	0.3273	17.92665144
LT34	3.1938	3.5609	0.3131	3.970195006
LT36	5.7151	1.2985	0.1749	0.295025853
LT39	8.7306	1.8913	0.1145	0.409710179
LT40	3.49066	5.6959	0.2864	9.294310191
LT41	4.136	1.8382	0.2417	0.816967901
LT44	4.2316	2.3433	0.2363	1.297630894
LT48	3.4504	7.3617	0.2898	15.70676643
LT49	2.5488	1.7797	0.3923	1.242675804
LT50	3.2593	6.0393	0.3068	11.19048400

4. CONCLUSION

This study applied the HVSR method to identify regional-scale variations in seismic site response across the Lake Toba region using microtremor data from 29 measurement stations. The resulting microzonation maps of predominant frequency (f_0), amplification factor (A_0), dominant period (T_0), and seismic vulnerability index (K_g) highlight zones with relatively higher and lower seismic susceptibility, particularly in relation to Quaternary alluvial deposits and consolidated volcanic formations. V_{s30} estimation and H/V inversion for shear-wave velocity (V_s) profiles were not conducted in this study due to the lack of independent subsurface constraints, such as borehole or active seismic data, which are required to reduce the non-uniqueness of HVSR inversion results. Therefore, the analysis focuses on robust HVSR-derived parameters (f_0 , A_0 , T_0 , and K_g) for regional-scale seismic hazard identification. Future studies integrating HVSR with complementary geophysical data are recommended for reliable V_{s30} -based site classification. Given the limited station density and the extensive spatial coverage of the study area, the results should be interpreted as a regional seismic hazard identification rather than a basis for site-specific engineering design or building regulations. Nevertheless, the findings provide an important preliminary framework for regional disaster risk mitigation planning and can serve as a reference for prioritizing areas where more detailed geophysical investigations and higher-resolution microzonation studies are required.

REFERENCE

- Akkaya, İ. (2015). The application of HVSR microtremor survey method in Yüksekova (Hakkari) region, Eastern Turkey. *Journal of African Earth Sciences*, *109*, 87-95.
- Aldiss, D. T., & Ghazali, S. A. (1984). The regional geology and evolution of the Toba volcano-tectonic depression, Indonesia. *Journal of the Geological Society*, *141*(3), 487-500.
- Alonso-Pandavenes, O., Bernal, D., Torrijo, F. J., & Garzón-Roca, J. (2023). A comparative analysis for defining the sliding surface and internal structure in an active landslide using the HVSR passive geophysical technique in Pujilí (Cotopaxi), Ecuador. *Land*, *12*(5), 961.
- Arrasyid, H., Maryanto, S., Wuryani, S. D., Santoso, D. R., & Subagiyo, A. (2024). Integration of Microtremor and PS-INSAR Analysis to Investigate the Susceptible Area in the Pronojiwo District (Indonesia) Following the 2021 East Java M6. 1 Earthquake. *Annals of Geophysics*, *67*(2), SE216-SE216.
- Asnawi, Y., Simanjuntak, A., Muksin, U., Rizal, S., Syukri, M. S. M., Maisura, M., & Rahmati, R. (2022). Analysis of microtremor H/V spectral ratio and public perception for disaster mitigation. *Geomate Journal*, *23*(97), 123-130.
- Chen, Z., Yao, H., Shao, X., Luo, S., & Yang, H. (2023). Detailed sedimentary structure of the Mianning segment of the Anninghe fault zone revealed by H/V spectral ratio. *Earthquake Research Advances*, *3*(3), 100232.
- Chen, S., Lei, J., & Li, Y. (2023). Microtremor recording surveys to study the effects of seasonally frozen soil on site response. *Sensors*, *23*(12), 5573.
- Eka Setiawan, R., Pramumijoyo, S., & Fathani, T. F. (2024). Site effect characterization and seismic vulnerability assessment using HVSR method in Yogyakarta region, Indonesia. *Geomate Journal*, *26*(101), 45-52.
- Gafoer, S., Amin, T. C., & Samodra, H. (1996). Geologic Map of Indonesia, Medan Sheet, Scale 1: 250.000. *Directorate General of Geology and Mineral Resources, Geological Research and Development Centre*.
- Gosar, A., Study on the applicability of the microtremor HVSR method to support seismic microzonation in the town of Idrija (W Slovenia). *Nat. Hazards Earth Syst. Sci.* *17*, 925-937 (2017). <https://doi.org/10.5194/nhess-17-925-2017>
- Grajales-Saavedra, F., Mojica, A., Ho, C., Samudio, K., Mejía, G., Li, S., ... & Muñoz, M. (2023). Horizontal-to-vertical spectral ratios and refraction microtremor analyses for seismic site effects and soil classification in the city of David, western Panama. *Geosciences*, *13*(10), 287.
- Grutas, R. N., Serrano, A. T., Tan, J. M. L. C., & Castro, R. A. F. (2025). Rapid Estimation of Vs30 Through Elitist Genetic Algorithm HVSR Inversion and Refraction Microtremor Data Analysis in the Greater Metro Manila Area and Leyte Province, Philippines. *Applied Sciences*, *15*(5), 2447.
- Hakim, L. (2019). Microtremor analysis for seismic microzonation and site response evaluation in urban areas. *Indonesian Journal of Geoscience*, *6*(3), 211-220.
- Hutchings, S.J., Mooney, W.D., The seismicity of Indonesia and tectonic implications. *Geochem. Geophys. Geosyst.* *22*, e2021GC009812 (2021). <https://doi.org/10.1029/2021GC009812>
- Konno, K., & Ohmachi, T. (1998). Ground-motion characteristics estimated from spectral ratio between horizontal and vertical components of microtremor. *Bulletin of the Seismological Society of America*, *88*(1), 228-241.
- Nakamura, Y. (1989). A method for dynamic characteristics estimation of subsurface using microtremor on the ground surface. *Railway Technical Research Institute, Quarterly Reports*, *30*(1).
- Nugroho, A., Santoso, D., & Prasetyo, H. (2023). Application of HVSR method for identifying sediment thickness and site response characteristics in urban areas. *Journal of Seismology and Earthquake Engineering*, *25*(2), 115-128.
- Simanjuntak, A., Muksin, U., Asnawi, Y., Rizal, S., & Wei, S. (2022). Recent Seismicity and Slab Gap Beneath Toba Caldera (Sumatra) Revealed Using Hypocenter Relocation Methodology. *Geomate Journal*, *23*(99), 82-89.
- Wibowo, N. B., Fathani, T. F., Pramumijoyo, S., & Marliyani, G. I. (2023). Microzonation of seismic parameters in geological formation units along the opak river using microtremor measurements. *Geomate Journal*, *25*(110), 208-219.
- Yulianto, T., & Yuliyanto, G. (2023). Microtremor data and HVSR method in the kaligarang fault zone Semarang, Indonesia. *Data in Brief*, *49*, 109428.